An Empirical Expression to Predict the Resonant Frequencies of Archimedean Spirals

Jerris W. Hooker, Vijaykumar Ramaswamy, *Student Member, IEEE*, Rajendra K. Arora, *Life Senior Member, IEEE*, Arthur S. Edison, Richard S. Withers, *Fellow, IEEE*, Robert E. Nast, and William W. Brey

***Abstract*—This paper presents an empirical formula to accurately determine the frequencies of the fundamental and higher order resonances of an Archimedean spiral in a uniform dielectric medium in the absence of a ground plane. The formula is based on method-of-moments simulations, which have been experimentally validated. This empirical formula is widely applicable to a broad range of spirals from thin-ring to disk-shaped (ratio of inner to outer radii 0 to 1), with ten or more turns.**

***Index Terms*—High-temperature superconducting (HTS) spiral resonators, nuclear magnetic resonance (NMR).**

I. Introduction

PLANAR SPIRAL coils are used in many applications as inductors or resonators. Examples of these applications include, but are not limited to, planar inductors [1], wireless power transfer [2], meta-materials [3], filters [4], and nuclear magnetic resonance (NMR) probe coils [5]. Specifically, when spirals are used as high-temperature superconducting (HTS) NMR probe coils, it is important to accurately predict not only the self-resonant frequency (SRF), but also the frequencies of the higher order modes. Many currently available formulas that describe the behavior of spirals are either only valid up to the SRF or are only applicable to a limited class of spiral designs. Presented in this study is an empirical expression that predicts the resonant frequencies of the modes with excellent accuracy for spirals with widely varying size, pitch, filling factor, and ratio of inner and outer radii. The expression is based on the simulated mode frequencies of spirals in a uniform dielectric medium.

The resonant frequencies of spirals have been investigated by others in several recent papers. In [6], an empirical formula was presented by Yun *et al.* for calculating the fundamental resonant frequency of a planar spiral. The formula they present is reasonably accurate in determining the SRF, but does not predict the higher order modes. In [7], Breitkeurtz and Henke solved a discretized transmission line model of a spiral to obtain the mode frequencies as well as the current distribution at the SRF and higher order modes. Other circuit models were introduced to model the behavior of spirals in [8] and [9], though the resonant behavior was not the focus. Even more recently, it was shown by Maleeva *et al.* [10] that when the inner radius approaches the outer radius, i.e., in the thin-spiral limit, the resonant current distribution and mode frequencies can be calculated analytically. In distinction to previous work, our project is to derive a simple formula for spiral resonances that covers the broadest possible range of geometric parameters. A detailed analysis of the effect of a dielectric substrate is outside of the scope of this study, but would be of great practical interest.

This work was organized into three stages. The first step was to validate a simulation approach by comparing simulated resonances to those measured experimentally or reported in the literature. This is described in Section III. The second step was to simulate the spectra for spirals with a wide range of parameters. Observations from this collection of spirals are given in Section IV. Details on a subset of the collection are given in Table I. Finally, in Section V, a formula was developed to fit the simulated resonances.

II. Background

A. Application

The motivation for this study is the authors' use of spiral resonators as a building block for NMR probes. NMR is an experimental technique that is widely used to identify compounds and their molecular structure. NMR provides a wealth of important information about molecular bonds that cannot be obtained by other methods, but it suffers from inherently low sensitivity. In NMR spectroscopy, samples are placed in a high magnetic field, which causes nuclei with nonzero spin to be resonant at frequencies proportional to this static magnetic field. At the heart of an NMR spectrometer is a sample probe that contains coils that generate uniform RF magnetic fields at the specific frequencies to excite and detect the NMR signals. Resonant coils with Q-values of several hundred are typically used to improve excitation efficiency and detection sensitivity. A further boost in sensitivity can be obtained from the use of HTS coils instead of normal metal coils [11]. These HTS coils are patterned out

Manuscript received November 04, 2014; revised January 27, 2015 and May 06, 2015; accepted May 09, 2015. This work was supported by the National Institutes of Health–National Institute of Biomedical Imaging and Bioengineering (NIH-NIBIB) under Grant 5R01EB009772. This work was performed at the National High Magnetic Field Laboratory, supported by the National Science Foundation (NSF) under Grant DMR-1157490, by the State of Florida, and by Agilent Technologies under a grant.

J. W. Hooker and W. W. Brey are with the National High Magnetic Field Laboratory, Florida State University, Tallahassee, FL 32310 USA (e-mail: wbrey@magnet.fsu.edu).

V. Ramaswamy and A. S. Edison are with the University of Florida and National High Magnetic Field Laboratory, Gainesville, FL 32610 USA.

R. K. Arora is with the Department of Electrical and Computer Engineering, Florida State University, Tallahassee, FL 32310 USA.

R. S. Withers is with Maxim Integrated, San Jose, CA 95134 USA.

R. E. Nast is with Out of the Fog Research, Mountain View, CA 94043 USA.

Color versions of one or more of the figures in this paper are available online at http://ieeexplore.ieee.org.

Digital Object Identifier 10.1109/TMTT.2015.2434814

TABLE I
DETAILS OF REPRESENTATIVE SIMULATED SPIRALS

	Mode number	Freq. Simulated (MHz)	Freq. Prediction (MHz)
Coil #1	1	706	717
$N = 20$	2	1658	1651
$r_i = 0.09$ mm	3	2591	2584
$r_o = 2.49$ mm	4	3524	3517
$P = 0.12$ mm	5	4455	4450
Coil #2	1	649	652
$N = 25$	2	1518	1507
$r_i = 0.12$ mm	3	2370	2362
$r_o = 2.12$ mm	4	3222	3217
$P = 0.08$ mm	5	4076	4072
Coil #3	1	415	406
$N = 5$	2	1071	1061
$r_i = 5.25$ mm	3	1722	1715
$r_o = 10.25$ mm	4	2388	2370
$P = 1.0$ mm	5	3053	3024
Coil #4	1	330	323
$N = 5$	2	811	806
$r_i = 5.5$ mm	3	1285	1289
$r_o = 15.5$ mm	4	1775	1772
$P = 2.0$ mm	5	2260	2255
Coil #5	1	202	201
$N = 10$	2	522	524
$r_i = 5.125$ mm	3	835	847
$r_o = 10.125$ mm	4	1159	1170
$P = 0.5$ mm	5	1480	1492
Coil #6	1	86	90
$N = 25$	2	271	264
$r_i = 5.01$ mm	3	438	438
$r_o = 6.01$ mm	4	617	612
$P = 0.04$ mm	5	787	786
Coil #7	1	224	229
$N = 10$	2	698	676
$r_i = 5.025$ mm	3	1128	1122
$r_o = 6.025$ mm	4	1581	1569
$P = 0.1$ mm	5	2020	2016
Coil #8	1	39.5	39.1
$N = 50$	2	102	102
$r_i = 5.025$ mm	3	163	165
$r_o = 10.025$ mm	4	226	227
$P = 0.1$ mm	5	289	290
Coil #9	1	22.1	23.2
$N = 10$	2	69.7	67.7
$r_i = 50.25$ mm	3	113	112
$r_o = 60.25$ mm	4	159	157
$P = 1.0$ mm	5	203	201

In this table the predicted data were obtained by the empirical formula described in Section V. The simulated values above were obtained from EM simulations described in Section III. In the simulations the ground plane was kept at a distance of at least 9 radii. All the spirals in the table above have a filling factor =50%. Each spiral was simulated for filling factors 10%, 20%, 30%, 40%, 50%, 60%, 70%, 80%, and 90%, with the same pitch and radii as stated in the table.

of thin-film yttrium–barium–copper–oxide ($YBa_2Cu_3O_{7-\delta}$ or YBCO) deposited as self-resonant structures on planar dielectric substrates such as sapphire [12]. Using self-resonant structures circumvents the need for lossy capacitors and other elements that would reduce the Q-values of the coils. Superconducting coils such as these typically possess matched Q-values ranging between 5000 and 20 000. Planar spiral resonators are a useful class of designs for these HTS probe coils. Spirals possess a strong magnetic dipole moment and they resonate at lower frequencies than designs that use interdigital capacitors because the conductor is long relative to the overall coil size. In these probes, the spiral coils are coupled and tuned via movable wire loops. A full description of this technology is given in [13].

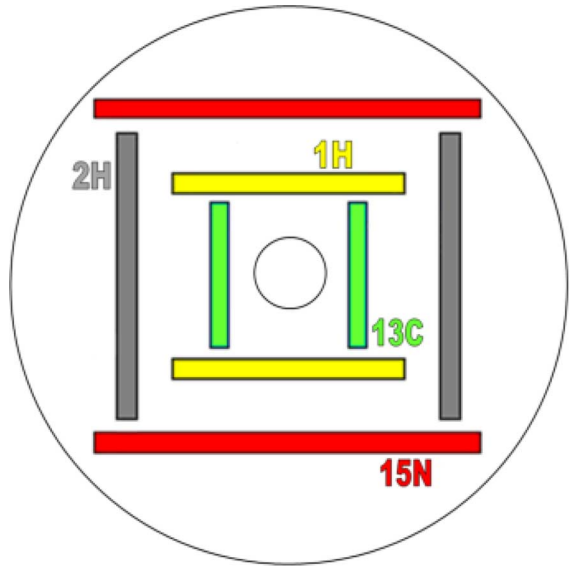

Fig. 1. Cross-section layout of an HTS NMR probe showing orthogonal nesting of Helmholtz pairs of resonators around a 1.5-mm sample [5].

NMR experiments require a uniform RF magnetic excitation field. To generate this field, a pair of coils is placed on opposite sides of the sample in a configuration similar to a Helmholtz pair. These coils must be very precisely tuned to resonate at the specific frequencies to which the nuclei of the isotope of interest will respond. The most informative NMR experiments excite multiple isotopes. Some of the most common are ^{1}H, ^{13}C, and ^{15}N. The NMR response of solvents with enriched levels of deuterium (^{2}H) is also typically used to regulate the static magnetic field to the 10^{-10} stability required over the duration of a signal-averaged experiment. In order to generate the necessary RF magnetic fields in an HTS probe, a separate pair of coils is included for each of these isotopes. These coil pairs are nested orthogonally around the sample to minimize interactions between the various channels. Fig. 1 shows a cross-sectional view of a typical coil arrangement within a probe.

B. Motivation

Effective design of HTS NMR probes requires a high level of control over where the fundamental and higher resonances of each coil occur. The fundamental spiral resonance should occur at the NMR resonance of the relevant isotope. The higher order modes of the spiral must also not interfere with the NMR resonances of higher frequency isotopes. The resonant frequency of ^{1}H nuclei is roughly four times that of ^{13}C nuclei and ten times that of ^{15}N nuclei so ^{15}N and ^{13}C coils with resonances in a harmonic series have modes at frequencies that will inter-

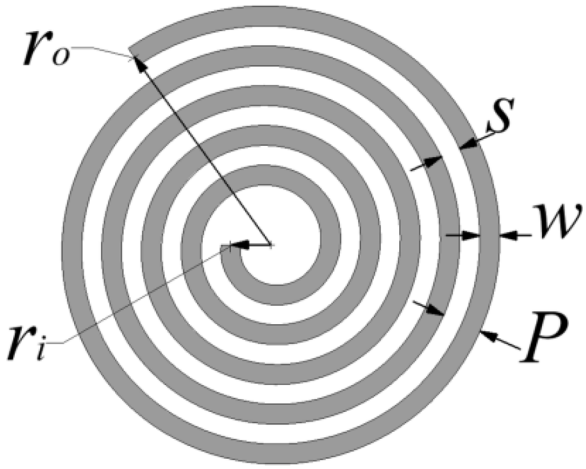

Fig. 2. Illustration of a spiral with relevant parameters annotated. These parameters include the wire width w, the turn spacing s, the pitch P, the inner radius r_i, and the outer radius r_o.

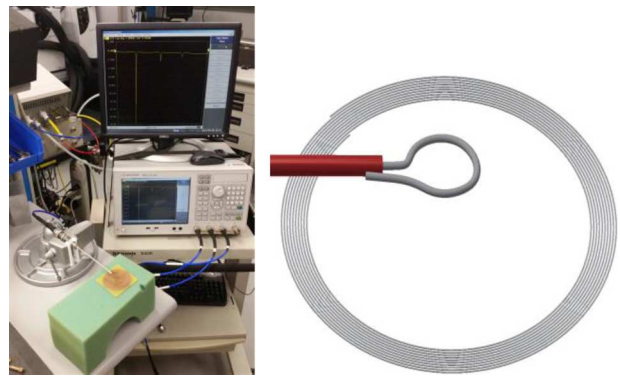

Fig. 3. *(left)* Photograph of the measurement setup. It consists of a network analyzer connected to a coupling loop. *(right)* Illustration of a spiral along with a coupling loop. The coupling loop is attached to the end of a coaxial cable, the other end of which is connected to a network analyzer. The details of this coil are listed in Table I as coil #7.

fere with the probe's ^{1}H channel. Method-of-moments simulation has been previously shown to be an effective way to predict the mode frequencies of spiral coils for NMR probes [11], but such simulations are relatively expensive and time consuming and by themselves provide little insight into the underlying relationships between the spiral parameters and the resonances. A simple and accurate predictive equation would accelerate the design process and provide coil designers with a tool to suitably adjust the mode spectrum.

A study of freestanding circular Archimedean spirals was chosen because they are the simplest of all spirals. However, HTS NMR coils, as well as many other applications for spiral inductors, use dielectric substrates to support the coil conductors. The effect of a dielectric substrate can be approximated to some extent by the use of an effective dielectric constant, as in [14]. HTS NMR coils are also typically rectangular rather than circular. The objective of this work is to develop a basic understanding of spiral resonance behavior using these simplified designs. It would be useful to extend our approach to include the effect of substrates and noncircular shapes.

III. Methods

A filamentary circular spiral is described in polar coordinates (r, θ) by the equation $r = r_i + \alpha\theta$, where r_i is the inner radius and α sets the distance between turns. A few other simple and interrelated parameters will be used to describe the spirals in this paper. These include the wire width w, the spacing between wires s, the number of turns N, and the outer radius r_o. To remove ambiguity, the inner radius is measured from the center of the conductor at the start of the first turn and the outer radius is measured from the center of the conductor at the end of the last turn. These parameters are depicted in Fig. 2 for the reader's convenience. It is also convenient to use the derived parameters of pitch $P = w + s = 2\pi\alpha$ and filling factor $F = w/P$.

The basic approach of this work was to use an efficient simulation process to evaluate the resonance frequencies of a collection of spirals and use the resulting data to determine relationships between the spiral parameters and the resonances. The spiral collection consisted of more than 80 different designs exhibiting filling factors ranging from 10% to 90%, numbers of turns varying between 5 and 50, ratios of inner and outer radii from 0.03 to 0.88, and a variety of pitch values. The SRF and the frequencies of the next five higher order modes were all determined for each spiral through simulation. The spiral spectra were then analyzed to characterize the deviation of the modes from a purely harmonic series. The spectra were also used to derive an empirical formula to predict frequencies of modes of spirals of arbitrary parameters.

A. Coupling to the Resonators

In this investigation, resonant frequencies were determined by measuring or simulating the reflection coefficient into a single loop loosely coupled to the spiral and excited by a 50-Ω source. When measuring the resonances by experiment, a single coupling loop connected to a vector network analyzer was used. The setup is shown in Fig. 3. The mutual inductance between the loop and the spiral induces some shift in the apparent resonant frequency. Froncisz *et al.* in [15] derived an expression for this shift, which is stated in (1) as follows:

$$f_{\text{measured}} = f_0 \left(1 - \frac{2\pi f_0 L_c}{Z Q_0}\right)^{-1/2}. \tag{1}$$

Here, f_0 represents the resonant frequency of the spiral in the absence of the coupling loop, f_{measured} is the observed resonant frequency under a "matched" condition, L_c is the inductance of the coupling loop, Q_0 is the quality factor of the coil, and Z is the impedance to which the coil is matched by the coupling loop. For high-Q devices matched to high impedances (i.e., loosely coupled to 50 Ω) through a coupling loop with small self-impedance L_c, the frequency shift is negligible. The measurement of the resonant frequencies could also have been made using two loops and observing the transmission coefficient, but the mutual inductance between the two coupling loops would also have created a shift in the measured frequency, as described in [16]. The spirals were placed at least nine radii from the ground plane so that resonance shifts due to eddy currents in the ground plane would be negligible. It can be noted that upper

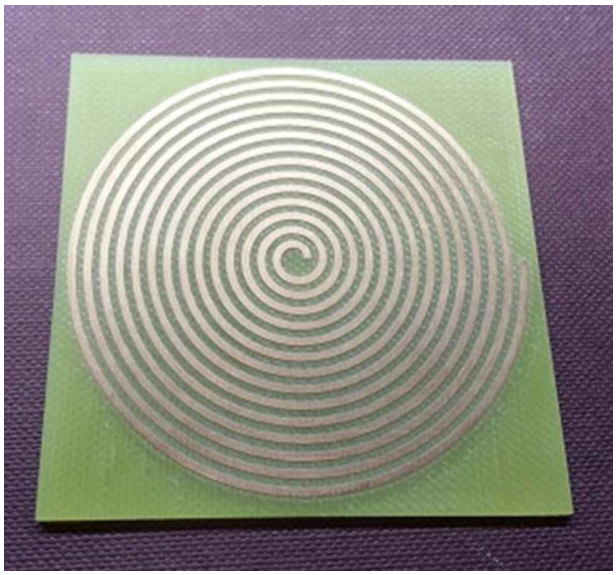

Fig. 4. Archimedean spiral used to verify the accuracy of simulations. The spiral was fabricated from a copper clad FR4 circuit board. Simulations of this device match well with measured experimental results.

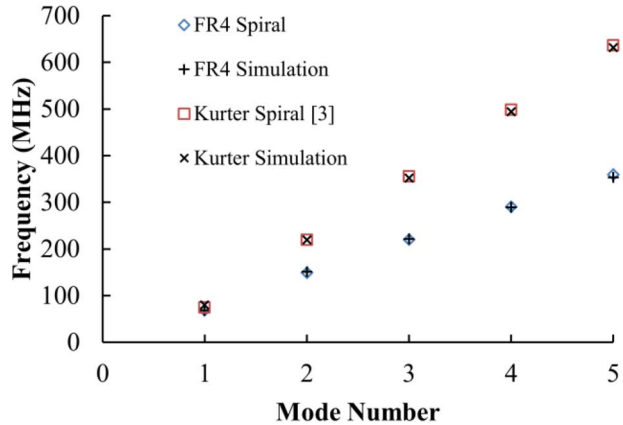

Fig. 5. Comparison of measured data against simulated results. The data include results reported by Kurter *et al.* in [3] and measured results from the spiral in Fig. 4, and the results from simulations of both spirals.

modes are largely unaffected by even a relatively nearby ground plane due to their small magnetic dipole moments.

B. Simulation

Simulations used to determine the resonant frequencies were performed using the Hyperlynx (Mentor Graphics) software package. Through routine modeling, it was observed that this package is very accurate in simulations of inductively coupled planar NMR probe coils.

The mode frequencies of two spiral resonators are then compared with experimental measurements to validate the simulation technique. In the first test, the spiral described by Kurter *et al.* was simulated and the obtained results were compared to the measurements reported in [3]. The frequencies reported in [3] are 74, 219, 355, 498, and 636 MHz. The results obtained through simulation are 80, 219, 352, 494, and 631 MHz. In a second test, an Archimedean spiral was patterned on an FR4 substrate, shown in Fig. 4, and measured its resonance frequencies for comparison to our simulations. These results from the Kurter spiral and those from the spiral on an FR4 substrate are given in Fig. 5. An exact value for the dielectric constant of the FR4 board was not available, but reported values for FR4 substrates range between 4.2 and 4.8. A value of 4.3 was used, which provided a good match between the SRF and the simulation. A single small pick-up loop was coupled to the spiral and the reflection coefficient was measured to determine the resonances. Modes were observed at 68, 149, 220, 290, and 359 MHz. The corresponding simulated modes were in close correspondence at 68, 151, 221, 289, and 353 MHz. Aside from the uncertainty in the dielectric constant of the FR4, the agreement between the simulations and measurements is at the level of 1%, which is sufficient for present purposes.

Using the verified simulation approach, a collection of more than 80 spiral resonators having a wide range of parameters were simulated up to the sixth resonant mode. The spiral from Fig. 4 is not included in this collection since its substrate would affect the results. Selected results are listed in Table I. This collection of spiral modes was used to develop and test the empirical formula in Section V. Subsets of this collection were used for the plots in Section IV.

IV. Observations

The modes observed in the studied spirals were analogous to the TEM modes seen in transmission line resonators: the number of maxima in the magnitude of the current along the conductor is equal to the mode number of the resonance. All spirals in this investigation were inductively coupled, which enforced the boundary condition that the current must be zero at each end. As a result, modes that required nonzero current at the ends of the spiral were not allowed.

The spiral from Fig. 3 (coil #7 in Table I) is chosen as an example to illustrate some of the general properties of planar spirals. Fig. 6 shows the resonance frequencies of the first eight modes of coil #7. This resonance behavior shows features commonly exhibited by the wide range of spirals that were simulated. Fig. 6 also includes, for comparison, the resonances of a uniform transmission line of the same physical length. As is well known, the spectrum of the uniform transmission line is harmonic, meaning that the frequency of the nth mode is exactly n times the SRF, where n is a natural number. In a mode plot such as Fig. 6, a trendline through the modes of a uniform transmission line will have a y-intercept of zero. The mode plot of the spiral is similar in having resonances that lie along a straight trendline. However, both the slope and y-intercept of the trendline are somewhat different from the uniform transmission line. The y-intercept of the spiral trendline is negative, which results in a lower SRF for the spiral by about 50% compared to the corresponding mode of the uniform transmission line. The slope of the spiral trendline is also greater than that for the uniform transmission line so the frequency gap between resonances for this spiral is about 4% larger than for a uniform transmission line. The variation in the slope of the spiral trendline appears to be related to the number of turns. In Fig. 7, the normalized slope of the spectrum has been plotted against the number of turns for the nine spirals of Table I. The quantity $(c/2L)$ was used to

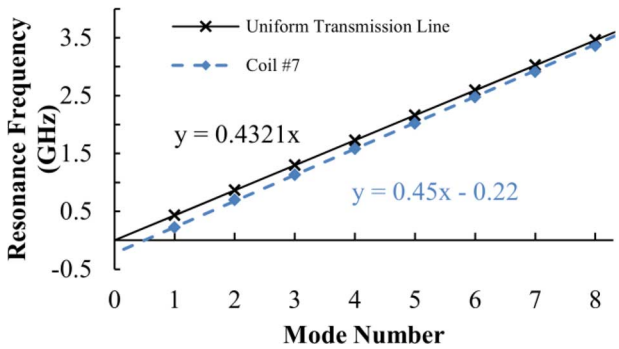

Fig. 6. Comparison between the modes of a harmonic transmission line and an Archimedean spiral resonator is shown. The conductor length of the spiral is the same as the length of the transmission line (347 mm).

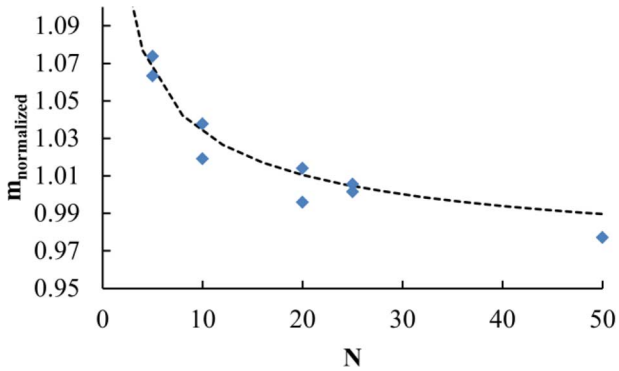

Fig. 7. Normalized slope of the mode spectrum depends on the number of turns. Spirals with roughly 30 and 40 turns have the same slope as a transmission line of the same length, while spirals with 5–30 turns were observed to have a greater slope and spirals with more turns, a smaller slope.

normalize each value, where c is the speed of light and L is the conductor length.

The quantity D is now introduced to describe the deviation from a harmonic spectrum. D is defined by (2) as follows, where b is the y-intercept of the trendline, and m is its slope:

$$D = \frac{b}{m}. \tag{2}$$

Since m will always be positive, the sign of D depends only on the sign of b. D was observed to be negative for each the Archimedean spirals in uniform media that were analyzed, and the SRF was observed to be consistently less than the SRF for a straight wire of the same length. Previously reported measurements indicate that, for the cylindrical helix in a uniform medium, D can be positive for some structures and mode frequencies are sometimes higher than for a straight transmission line of equivalent length [17].

An expression for the quantity D is important because it allows a coil designer to quantify the type of mode spectrum needed for a particular design. Based on simulations of the spirals in Table I among others, it was observed that D is primarily determined by the ratio of the inner radius r_i to the outer radius r_o, and to a lesser extent by the filling factor F and pitch P. A graph depicting the relationship between D and r_i/r_o for different values of F is shown in Fig. 8. Each spiral investigated was simulated with nine different filling factors ranging from 10% to 90%. As the filling factor was increased from 10% to 90%, D was observed to decrease, as is shown in Fig. 8. Based on values of D obtained from the simulated spirals just described, an empirical expression was developed to model the dependence of D on the various parameters of the spiral. Equation (3) relates D directly to the filling factor, scaled pitch, and ratio of the radii,

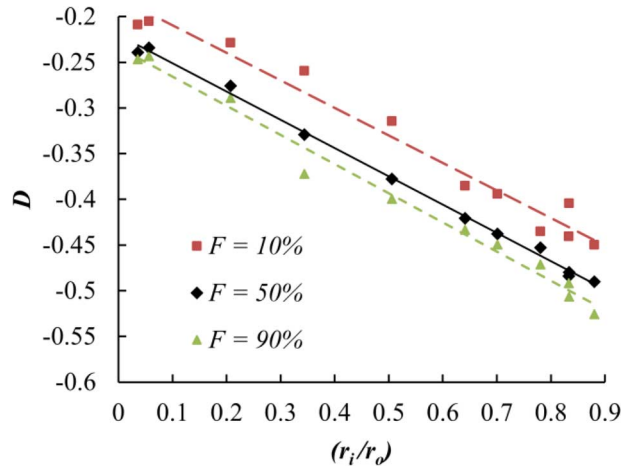

Fig. 8. Deviation from harmonic behavior seen in a variety of circular Archimedean planar spirals. These spirals have a wide range of pitch and number of turns. It is clear that D depends primarily on the ratio of inner and outer radii.

$$D = -\left((0.29 + 0.043\,F)\left(\frac{r_i}{r_o}\right) + 0.22\right) \times \left((F - 0.5)\left(2.65\left(\frac{P}{r_0}\right) + 0.03\right) + 1\right). \tag{3}$$

All coil parameters were defined in Section III. Note that for a filling factor of 50%, D is independent of the pitch.

V. Calculation of Resonant Frequencies

A. Empirical Expression

An expression to calculate the resonant frequencies of an Archimedean spiral was generated by curve fitting the simulated resonances of a collection of spirals, some of which are detailed in the Table I. The expression is given in (4) as follows:

$$f_n(\text{Hz}) = \left(\frac{v}{2L}\right)(0.24N^{-0.46} + 0.95)(n + D). \tag{4}$$

In (4), n is the mode number, N is the number of turns in the spiral, and v is the velocity of electromagnetic waves in the surrounding medium. The expression for D is given by (3). Since all the parameters in (4) are either unitless or participate in simple ratios, any consistent choice of length units can be used. It is straightforward to derive (5) as follows, which gives the length L of an Archimedean spiral:

$$L = \left(\frac{r_o}{2}\right)\sqrt{\frac{r_o^2}{\alpha^2} + 1} + \left(\frac{\alpha}{2}\right)\ln\left(\frac{r_o}{\alpha} + \sqrt{\frac{r_o^2}{\alpha^2} + 1}\right) - \left(\frac{r_i}{2}\right)\sqrt{\frac{r_i^2}{\alpha^2} + 1} - \left(\frac{\alpha}{2}\right)\ln\left(\frac{r_i}{\alpha} + \sqrt{\frac{r_i^2}{\alpha^2} + 1}\right). \tag{5}$$

If the spiral is supported by a dielectric substrate, the velocity v can be calculated by dividing the speed of light by the square

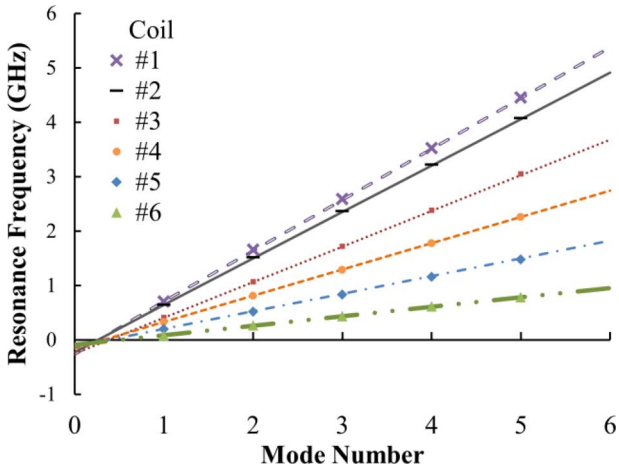

Fig. 9. Comparison between the simulated frequencies and those predicted by (7). Coil details are included in Table I.

root of an effective dielectric constant [18]. For thick substrates, a good approximation for an effective dielectric constant can be obtained from (6) as follows:

$$\varepsilon_{\text{eff}} = \frac{(\varepsilon_r + 1)}{2}. \tag{6}$$

When the substrate thickness is small, the modes may not all be affected equally and a more rigorous determination of effective dielectric constant will be required. The threshold of thickness is governed by the parameters of the spiral and the amount electric field fringing that occurs.

The empirical formula in (4) produced an accurate prediction of the resonance frequency for each of the spirals simulated. The average error seen across more than 480 resonant frequencies gathered from 81 different spirals was about 0.87%, the median error was 0.56%. Roughly 46% of the resonance frequencies were predicted to within 0.5% error and about 93% of frequencies were predicted to within less than 2% error.

In the case where $F = 50\%$, (3) takes on a simpler form. When (3) and (4) are combined under this condition, the following equation is produced:

$$f_n(\text{Hz}) = \left(\frac{v}{2L}\right)(0.24N^{-0.46} + 0.95) \times \left(n - \left((0.31)\left(\frac{r_i}{r_o}\right) + 0.22\right)\right). \tag{7}$$

The level of accuracy of (7) is shown in Fig. 9, where the first five resonances simulated for six different spirals with 50% filling factor are plotted along with the prediction curves generated from (7). As shown, there is excellent agreement between the two.

The proposed formula was applied to three different Archimedean spirals reported in the literature by other investigators. Table II contains the data showing how accurately the resonance frequencies were predicted. Specifically, the percent error for the resonant frequencies determined by the empirical formula relative to those measured by experiment is given. The example from [3] and SR2 reported in [18] were modeled very accurately. These two coil examples are both fabricated from a superconducting film. The remaining example, SR1 from [18], was not modeled nearly as well. In all three examples, the effective dielectric constant was determined using (6). The SR1 example illustrates the limitation of (6) when the substrate is thin relative to the spiral dimension. In the two well-modeled examples, the substrate thickness is at least 20% of the spiral width $(r_o - r_i)$. In the case of SR1, the substrate thickness is less than 5% of this value.

TABLE II
COMPARISON TO PUBLISHED DESIGNS

mode	% error for SR1 in [18] $\varepsilon_r = 3.48$	% error for SR2 from [18] $\varepsilon_r = 11.45$	% error for example in [3] $\varepsilon_r = 4.53$*
1	16%	0.99%	0.58%
2	15%	1.3%	3.2%
3	11%	0.83%	1.7%
4	8.6%	1.3%	2.5%
5	6.7%	1.0%	2.1%

This table shows the accuracy with which the proposed formula predicts the resonance frequencies of spirals that have been reported by other investigators. The ratio of the frequency predicted by the empirical formula to the frequency measured by the investigators is reported for each of the first 5 modes for the three examples. Accuracy was excellent in the case of the 2 superconducting spirals but significantly worse for SR1 which was fabricated on a copper clad PCB. *This dielectric constant was obtained from [19] as none was reported in [3]. This value represents the average of the permittivity values perpendicular and parallel to the anisotropy axis.

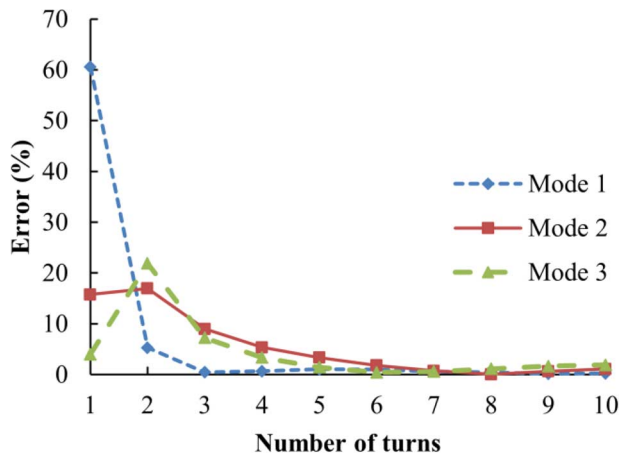

Fig. 10. Percent error in the first three modes of ten different spirals. They all have the same pitch, wire width, and outer radius, but the number of turns varies from one to ten.

B. Limitations of Empirical Formula

One of the limits of validity of (4) and (7) is when the spiral has less than ten turns. Consideration of a collection of spirals with the same pitch, wire width, filling factor, and outer radius demonstrates the few-turn limit, as shown in Fig. 10. Only the number of turns and inner radius are varied. The ten-turn spiral in this set is described in Table I as coil #5. The first three modes of the spirals were simulated, and then they were compared to the result of the empirical formula to calculate the associated error. The number of turns was decreased by removing turns from the center. As this occurred, the error increased. When fewer than five turns were used, the error increased significantly,

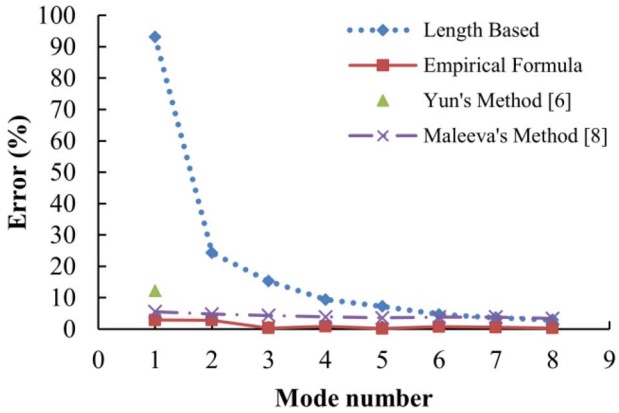

Fig. 11. Error associated with predicting the mode frequencies by four different methods. A length-based approximation, the method presented by Yun *et al.* in [6], the method presented by Maleeva *et al.* in [10], and a new empirical formula are all used to predict the resonant frequencies of a spiral. The empirical formula presented here maintains a consistently low level of error.

to as much as 60% when only one turn was present. The decreased accuracy of (4) for fewer than ten turns is not surprising. When sufficiently many turns are present, wave propagation is influenced by the effect of neighboring turns. When only one turn is present, the resonator approximates a uniform transmission line and has a nearly harmonic spectrum. However, for a single-turn spiral with r_i approximately equal to r_o, (3) predicts a large magnitude for D, while in actuality, D for a single-turn spiral is close to zero. While accurate results may be possible for some spirals with fewer than ten turns, this empirical formula cannot be recommended for those structures. Spiral resonators in NMR probes typically have more than ten turns.

The accuracy of (4) beyond about ten modes has not been explored. Very high-order modes are difficult to measure, both in simulation and by experiment, because their RF magnetic fields fall off rapidly with distance.

C. Comparison to Other Methods

In Fig. 11, the results of four different methods for predicting the resonances for the spiral of Fig. 3 (coil #7) are shown for comparison. The first method, calculating the resonant frequencies based solely on the conductor length, was only accurate for the highest modes. The next method, the one presented by Yun in [6], predicted the SRF with an accuracy of about 12%, but was not intended for use for higher order modes. The method presented by Maleeva *et al.* in [10] was derived from first principles for spirals with $r_i \approx r_o$ and performed very well for coil #7. As noted in [10], thin ring-shaped spirals exhibit a ratio of resonant frequencies of approximately $f_1 : f_2 : f_3 : \cdots : f_n = 1 : 3 : 5 : \cdots : (2n-1)$. Applying (2) to this mode spectrum results in value of $D = -0.5$, just as Fig. 8 and (3) predict will be observed for thin spirals. The empirical formula presented here exhibited consistently low error and is highly effective for a wide class of Archimedean spirals.

VI. Discussion

The utility of the empirical formula can be best illustrated with an example. The NMR frequency of the ^{15}N isotope at 14.1 T occurs at 61 MHz. Spiral resonator "Design 1" for ^{15}N was designed to operate with its fundamental resonance at 60 MHz,

TABLE III
Details of Example Spiral Designs

	Design 1	Design 2
N	72	42
r_i	2.16 mm	4.30 mm
r_o	4.91 mm	4.98 mm
P	0.019 mm	0.0164 mm
F	50%	50%

This table lists the parameters which describe the two spiral designs used in section VI. Design 1 suffers from modes that happen to occur at frequencies that are important to avoid. Design 2 was specifically designed using the presented techniques to avoid this problem.

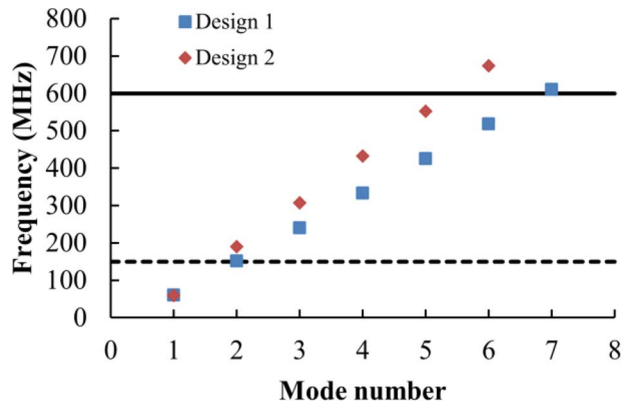

Fig. 12. Resonances of the two designs described in Table III. Also depicted are horizontal lines representing the frequencies where interference with the ^{1}H and ^{13}C resonances would occur. The modes for Design 1 overlap both of these frequencies, while the modes for Design 2 avoid them both.

however, additional resonances were found at 151, 240, 333, 425, 518, and 610 MHz. The additional resonances at 151 and 610 MHz are very close to the resonant frequencies for ^{13}C (151 MHz) and ^{1}H (600 MHz) at 14.1 T, and would be expected to degrade the performance of those channels. This particular coil consisted of 72 turns and a filling factor of 50%. The value of N was chosen to achieve the desired frequency given the outer radius. The wire width and spacing were both 0.019 mm, the inner radius was 2.16 mm, and the outer radius was 4.91 mm. These data are listed in Table III.

By using the empirical equation and data presented above, it was possible to redesign the coil to move the higher order resonances further away from the ^{13}C and ^{1}H frequencies. The design requirement may now be reframed as a resonator that has its fundamental frequency at approximately 60 MHz with the upper modes roughly 120 MHz apart. This corresponds to a value of -0.5 for D. According to Fig. 8, this occurs when the ratio of the radii is approximately 0.9. If a similar outer radius of 4.98 mm is used, then the appropriate pitch is determined to be 0.0164 mm, from (3), assuming that the length is the same as that for a transmission line that resonates at 120 MHz. The corresponding inner radius is 4.3 mm and the number of turns is 42. The predicted resonances according to (7) for "Design 2" are 61, 183, 304, 426, 547, and 669 MHz. Design 2 was simulated, and confirmed the resonance frequencies at 59, 190, 307, 432, 552, and 673 MHz. It is important to note that Design 2 has no modes near the ^{1}H or ^{13}C frequencies, making it a viable design. This characteristic is illustrated in Fig. 12, where the frequencies of the modes have been plotted together with

horizontal lines representing the resonances of the ^{13}C and ^{1}H isotopes. Minor adjustments can be made easily at this stage to fine tune the fundamental frequency. In this example, (3) and (7) were used to design a spiral that had the desired fundamental mode, but would not interfere with other channels, without the need for cut-and-try techniques or time-consuming simulations.

VII. Conclusion

A new empirical model has been presented in this paper that can be applied to Archimedean spirals very easily with good accuracy and will advise designers on the appropriate changes to make in order to produce the desired spectrum of resonant frequencies. The median error observed was approximately 0.56% and the mean was 0.87%. Over 99% of all predictions showed less than 5% error. The quantity D has also been introduced to describe the deviation from a harmonic spectrum exhibited by a spiral. The effect that adjusting the different parameters has on D is also discussed. Specifically, adjusting the ratio of inner and outer radii of spirals was determined to have the most significant effect on this amount of deviation from a harmonic spectrum. The information presented will be useful in designing spirals with resonant frequencies at very specific locations, which will reduce the need for cut-and-try techniques.

References

[1] C. C. Chen, C. Lin, and Y. T. Cheng, "Model to determine the self-resonant frequency of micromachined spiral inductors," *Appl. Phys. Lett.*, vol. 89, pp. 103521-1–103521-3, Sep. 2006.

[2] W. Wei, Y. Kawahara, N. Kobayashi, and T. Asami, "Characteristic analysis of double spiral resonator for wireless power transmission," *IEEE Trans. Antennas Propag.*, vol. 62, no. 1, pp. 411–419, Jan. 2014.

[3] C. Kurter *et al.*, "Superconducting RF metamaterials made with magnetically active planar spirals," *IEEE Trans. Appl. Supercond.*, vol. 21, no. 3, pp. 709–712, Jun. 2011.

[4] G. Zhang, F. Huang, and M. J. Lancaster, "Superconducting spiral filters with quasi-elliptic characteristic for radio astronomy," *IEEE Trans. Microw. Theory Techn.*, vol. 53, no. 3, pp. 947–951, Mar. 2005.

[5] V. Ramaswamy *et al.*, "Development of a 13C-optimized 1.5-mm high temperature superconducting NMR probe," *J. Magn. Reson.*, vol. 235, pp. 58–65, Oct. 2013.

[6] H.-C. Yun, G. Lee, and W. S. Park, "Empirical formulas for self resonance frequency of Archimedean spiral coils and helical coils," in *Proc. IEEE Antennas Propag. Soc. Int. Symp.*, Jul. 2012, pp. 1–2.

[7] B. Breitkreutz and H. Henke, "Calculation of self-resonant spiral coils for wireless power transfer systems with a transmission line approach," *IEEE Trans. Magn.*, vol. 49, no. 9, pp. 5035–5042, Sep. 2013.

[8] K. Y. Lee, S. Mohammadi, P. K. Bhattacharya, and L. P. B. Katehi, "Compact models based on transmission-line concept for integrated capacitors and inductors," *IEEE Trans. Microw. Theory Techn.*, vol. 54, no. 12, pp. 4141–4148, Dec. 2006.

[9] Y. G. Ahn, S. K. Kim, J. H. Chun, and B. S. Kim, "Efficient scalable modeling of double-π equivalent circuit for on-chip spiral inductors," *IEEE Trans. Microw. Theory Techn.*, vol. 57, no. 10, pp. 2289–2300, Oct. 2009.

[10] N. Maleeva *et al.*, "Electrodynamics of a ring shaped spiral resonator," *J. Appl. Phys.*, vol. 115, pp. 064910-1–064910-8, 2014.

[11] W. W. Brey *et al.*, "Design, construction, and validation of a 1-mm triple-resonance high-temperature-superconducting probe for NMR," *J. Magn. Reson.*, vol. 179, pp. 290–293, Apr. 2006.

[12] P. Berberich, B. Utz, W. Prusseit, and H. Kinder, "Homogeneous high quality $YBa_2Cu_3O_7$ films on 3″ and 4″ substrates," *Phys. C, Supercond.*, vol. 219, pp. 497–504, Jan. 1994.

[13] V. Ramaswamy *et al.*, "Microsample cryogenic probes: Technology and applications," *EMagRes*, vol. 2, pp. 215–228, Jun. 2013.

[14] S. Ramo, J. R. Whinnery, and T. Van Duzer, *Fields and Waves in Communication Electronics*. New York, NY, USA: Wiley, 1965, ch. 8, p. 412.

[15] W. Froncisz, A. Jesmanowicz, and J. Hyde, "Inductive (flux linkage) coupling to local coils in magnetic resonance imaging and spectroscopy," *J. Magn. Reson.*, vol. 66, pp. 135–143, Jan. 1986.

[16] G. Ghamsari, J. Abrahams, S. Remillard, and S. M. Anlage, "High-temperature superconducting spiral resonator for metamaterial applications," *IEEE Trans. Appl. Supercond.*, vol. 23, pp. 1500304-1–1500304-4, Jun. 2013.

[17] F. Engelke, "Electromagnetic wave compression and radio frequency homogeneity in NMR solenoidal coils: Computational approach," *Concepts Magn. Reson.*, vol. 15, pp. 129–155, Jun. 2002.

[18] N. Maleeva *et al.*, "Electrodynamics of a planar Archimedean spiral resonator," *Arxiv:1411.5823, Cond-mat.supr-con*, Nov. 2014.

[19] J. Krupka, K. Derzakowski, M. Tobar, J. Hartnett, and R. G. Geyer, "Complex permittivity of some ultralow loss dielectric crystals at cryogenic temperatures," *Meas. Sci. Technol.*, vol. 10, pp. 387–392, May 1999.

Jerris W. Hooker, photograph and biography not available at the time of publication.

Vijaykumar Ramaswamy (S'09–GSM'14), photograph and biography not available at the time of publication.

Rajendra K. Arora (S'64–M'65–SM'74–LSM'02), photograph and biography not available at the time of publication.

Arthur S. Edison, photograph and biography not available at the time of publication.

Richard S. Withers (S'78–M'78–SM'97–F'09), photograph and biography not available at the time of publication.

Robert E. Nast, photograph and biography not available at the time of publication.

William W. Brey, photograph and biography not available at the time of publication.